Damage Identification in Concrete Gravity Dams Using Static and Dynamic Measurement Data

N.T. Le[1,*], D.P. Thambiratnam[2], A. Nguyen[3], T.H.T. Chan[2]
[1] National University of Civil Engineering, Hanoi, Vietnam
[2] Queensland University of Technology, Brisbane, Australia
[3] University of Southern Queensland, Springfield, Australia
* Corresponding author
Email: thachln2@nuce.edu.vn, d.thambiratnam@qut.edu.au, andy.nguyen@usq.edu.au, tommy.chan@qut.edu.au

ABSTRACT: Dams and reservoirs are important elements of civil infrastructure as they play critical roles in irrigation, flood control and electricity generation. Historically, dam failures have led to catastrophic loss in lives and properties. The need to monitor structural performance and detect the onset of damage in these structures using structural measurement data is thus evident, yet the relevant research has been limited. This paper presents an approach for damage detection of concrete gravity dams based on changes in static deflection and modal parameters. Theoretical formula of the static deflection change with regard to the damage characteristics taken into account both flexural and shear effects is developed. Based on this, the research shows that changes in the static deflection follow certain patterns that can be used to locate and quantify the damage in concrete gravity dams. The proposed static damage detection concept is then incorporated with vibration measurements through the modal flexibility to assess the damage. Numerical studies in this study show that the proposed approach is promising in detecting seismic cracks that are often a common damage type in real concrete dams.

KEY WORDS: Damage identification; Concrete gravity dams; Static deflection change; Modal flexibility change, Vibration characteristics.

1 INTRODUCTION

Dams and reservoirs are key elements of civil infrastructure systems due to their important roles in irrigation, flood control and electricity generation. Historically, the failures of these structures have led to catastrophic loss in lives and properties [1]. The need to monitor structural performance and detect the onset of damage in these important structures to ensure their integrity and longevity, and prevent subsequent failures is thus evident. In recent decades, structural health monitoring (SHM) has emerged as a feasible technique for these purposes by using on-structure, non-destructive sensing systems [2]. In fact, dams are among the most important structures for the mandated application of SHM as can be seen in dam safety regulations of many countries.

The existing damage identification (DI) methods for civil engineering structures can be classified into different categories, such as dynamic methods, static methods and static-dynamic methods, depending on the type of structural measurement data being used. The fundamental idea of the DI techniques is that when damage in a structure becomes reasonably significant, it can cause changes in its properties (mass, stiffness, and damping), and these in turn will cause detectable changes in the vibration characteristics (such as natural frequencies and mode shapes) [3, 4] and static responses (such as deflection and strains) [5]. Therefore, by assessing changes in basic structural response such as natural frequencies, mode shapes and static deflections one can assess structural damage with regard to its presence, location and severity. Based on this fundamental idea, a variety of DI methods have been proposed for civil engineering structures including bridges [6-9], shear building [10, 11], asymmetrical buildings [12], concrete dams [13, 14], and beam-type structures [5, 15-17], to name a few.

The selection of suitable DI methods for a structure not only depends on the sensitivity of the selected features to the structural damage, but also on the availability of the monitoring data. For concrete gravity (CG) dams, static deflection has long been one of the most available and reliable structural responses for structural health monitoring and assessment [18]. In addition, as many of the large dams in the world are subjected to earthquakes, vibration measurement has been a viable source of long-term/continuous monitoring data from vibration sensing and strong earthquake monitoring systems [14, 19]. Both static and dynamic measurements should be considered for damage identification in CG dams. However, the relevant research in the literature has been limited [20].

In this paper, a DI approach for CG dams based on the changes in static deflection and/or modal flexibility is proposed. First, a theoretical relationship between the static deflection change and the damage characteristics is developed using Virtual work method for Timoshenko beams. Based on this, the damage locating and quantification concepts are presented. Next, modal flexibility change constructed from vibration measurements is incorporated with the proposed static DI concept to provide a static-dynamic-based capacity in assessing the damage. Numerical studies are then presented for a typical CG dam model to verify the efficacy of the proposed approach. The paper then concludes with some final remarks.

2 THEORY

2.1 Damage Identification Concepts of CG Dams from Static Deflection Change

Consider a typical homogeneous CG dam section with the dimensions as shown in Figure 1-a. The dam profile can be idealized as a Timoshenko cantilever beam with varying cross section (Figure 1-b). The area *A(z)* and the second moment of

area *I(z)* of the dam section at an arbitrary elevation *z* can be expressed by:

$$A(z) = A_b\left(1 - \psi_b \frac{z}{H}\right) \tag{1}$$

$$I(z) = I_b\left(1 - \psi_b \frac{z}{H}\right)^3 \tag{2}$$

where, $A_b = 1 \times B_b$ and $I_b = (1/12) \times 1 \times B_b^3$ are the area and moment of inertia of the dam section at its base, respectively; H is height of the dam; $\psi_b = (B_b - B_t)/B_b$ is a scalar representing the beam cross section change.

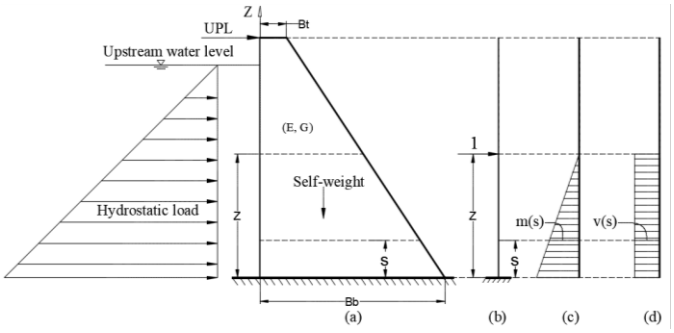

Figure 1. (a) Configuration of typical CG dam section, (b) Simplified cantilever under virtual UPL, (c) and (d) Virtual bending moment and shear force diagrams

The lateral deflection of the idealized beam under an arbitrary lateral static load in the undamaged state can be formulated from the principle of Virtual Work method for Timoshenko beams as follows:

$$u(z) = \int_0^H \frac{M(s)\ m(s)}{EI_b\left(1 - \psi_b \frac{s}{H}\right)^3} ds + \int_0^H \frac{V(s)\ v(s)}{\eta G A_b\left(1 - \psi_b \frac{s}{H}\right)} ds \tag{3}$$

where, M and V are the moment and shear force of the beam under the real static loads; m and v denote the virtual moment and shear forces under a virtual horizontal unit point load acting at elevation z; E is the Young's modulus, $G = E/[2(1+\nu)]$ is the shear modulus, ν is Poisson's ratio of the concrete material; η is the shear correction factor.

The first integration in equation (3) represents the deflection under pure bending mode, while the second integration represents the deformation under pure shear condition.

As moment and shear distributions of statically determinate beams do not depend on the cross-sectional stiffness, the equations of *m(s)* and *v(s)* of the dam as a cantilever beam can be given by Figure 1-c, d):

$$m(s) = \begin{cases} z - s\ ; & 0 \le s \le z \\ 0\ ; & s > z \end{cases} \tag{4}$$

$$v(s) = \begin{cases} 1\ ; & 0 \le s \le z \\ 0\ ; & s > z \end{cases} \tag{5}$$

On substitution of equations (4) and (5) to equation (3), it turns to:

$$u(z) = \frac{H^3}{EI_b}\int_0^z \frac{M(s)\ (z-s)}{\left(H - \psi_b s\right)^3} ds + \frac{H}{\eta G A_b}\int_0^z \frac{V(s)}{H - \psi_b s} ds \tag{6}$$

In the damaged state, assuming the dam is subjected to a single damaged region $a \le x \le a + b$ (Figure 2-a), with the corresponding stiffness reduction of α ($0 \le \alpha < 1$), i.e. the remaining bending and shear stiffness in the damaged region are (1-α)*EI* and (1-α)*GA*, respectively. From the Virtual Work method, the damage-induced deflection difference, or deflection change (*DC*), of the dam along the measurement points can be formulated by:

$$DC(z) = u^d - u^h = \begin{cases} 0 & ;\quad z \le a \\ \dfrac{\beta H^3}{EI_b}\displaystyle\int_a^z \frac{M(s)(z-s)}{\left(H - \psi_b s\right)^3} ds + \frac{\beta H}{\eta G A_b}\int_a^z \frac{V(s)}{H - \psi_b s} ds\ ; & a \le z \le a + b \\ \dfrac{\beta H^3}{EI_b}\displaystyle\int_a^{a+b} \frac{M(s)(z-s)}{\left(H - \psi_b s\right)^3} ds + \frac{\beta H}{\eta G A_b}\int_a^{a+b} \frac{V(s)}{H - \psi_b s} ds\ ; & z \ge a + b \end{cases} \tag{7}$$

where, u^d and u^h are the deflections of the dam in the damaged and undamaged states, respectively; β is a damage severity derivative defined as follows:

$$\beta = \frac{\alpha}{1 - \alpha} \tag{8}$$

It can be observed from equation (7) that the *DC(z)* plot encompasses a zero portion in the first undamaged region $0 \le z \le a$, then increases by a high order function in the damaged region $a \le z \le a + b$, before linearly increases in the second undamaged region $z \ge a + b$ (Figure 2-b). Therefore, by observing a measured *DC* plot, the damaged region can be detected within the zero and the linearly portions. This distinctiveness is used in the present study to locate the damage in CG dams.

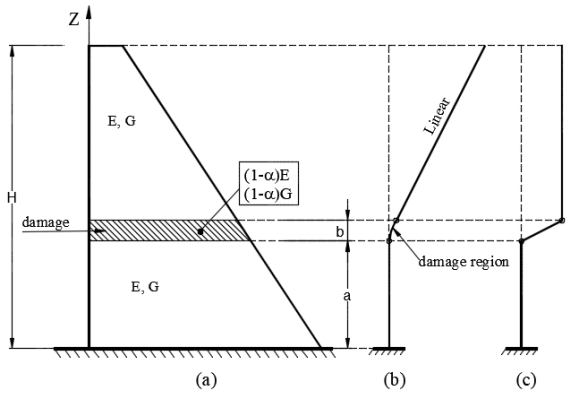

Figure 2. (a) Single damage scenario, (b) Deflection change pattern, (c) Slope of deflection change pattern

It is noted that the *DC* formula of cantilever Euler-Bernoulli beams presented in Le *et al*, [16] is a special case of the above developed *DC* pattern since it did not take into account shear effect and cross sectional variation. In addition, when the bending moments in Eq. (7) are neglected, the *DC* becomes a constant function in the region $z \ge a + b$, which is relevant to the *DC* pattern of shear building reported by Koo *et al*, [10]. Therefore, the developed *DC* function for Timoshenko cantilever beams in equation (7) covers the two special cases for purely bending and purely shear structures.

By differentiating equation (7) with respect to *z*, the slope of the deflection change (*SDC*) of the linear portion of the *DC*(*z*) plot can be given by:

$$SDC = \frac{d}{dz}DC(z) = \beta\left[\frac{H^3}{EI_b}\int_a^{a+b}\frac{M(s)}{\left(H-\psi_b s\right)^3}ds\right] \quad (9)$$
$$+ 0 = \beta.SDC^{50\%} \quad (z \geq a+b)$$

Or,

$$SDC = \beta.SDC^{50\%} \quad (z \geq a+b) \quad (10)$$

where, $SDC^{50\%}$ is a scalar function within the square brackets in equation (9), containing the undamaged material Young's modulus *E*, the damage location identifiers (*a*, *b*), and the geometrical dimensions of the dam section. It is evident from equation (10) that $SDC^{50\%}$ equals the measured *SDC* when $\beta = 1$, or $\alpha = 50\%$ as can be deduced from equation (9). This means $SDC^{50\%}$ is the measured *SDC* of the cantilever beam when it subjected to damage at a $\leq z \leq a+b$ with a 50% damaged severity. This explains the superscription 50% of the $SDC^{50\%}$ term. In addition, equation (10) shows that the measured *SDC* differs from $SDC^{50\%}$ by a scalar (β). Therefore, $SDC^{50\%}$ can represent a baseline *SDC*.

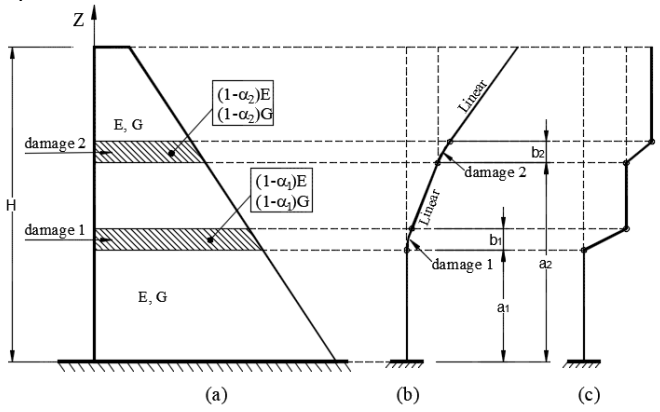

Figure 3. (a) Double damage scenario, (b) Deflection change pattern , (c) Slope of deflection change pattern

When the dam experiences damage at two different regions (Figure 3-a), for example multiple cracked zones after an earthquake, with the damage location identifiers (a_i, b_i) and the damage severities α_i (i=1,2), the *DC* function of the dam can be formulated analogously with the single damage case. It comprises of a zero portion in the undamaged region $0 \leq z \leq a_1$, two high order functions in the damaged regions (a_i, a_i+b_i), and two linear portions in the undamaged regions (a_1+b_1,a_2) and z $\geq a_2 + b_2$ (Figure 3-b). The corresponding slopes of the two linear portions of the *DC(z)* plot can be presented by (Figure 3-c):

$$SDC_1 = \beta_1 SDC_1^{50\%};\ a_1 + b_1 \leq z \leq a_2$$
$$SDC_2 = SDC_1 + \beta_2 SDC_2^{50\%};\ z \geq a_2 + b_2 \quad (11)$$

where, the baseline *SDC* scalars are given by:

$$SDC_i^{50\%} = \frac{H^3}{EI_b}\int_{a_i}^{a_i+b_i}\frac{M(s)}{\left(H-\psi_b s\right)^3}ds;\ i = 1,2 \quad (12)$$

The scalar $SDC^{50\%}$ can be calculated either numerically from an updated finite element model, or by expanding equation (12) under a specific static loading condition. From equations (10) and (11), the damage severity derivatives are then calculated from the following equations:

$$\beta_1 = \frac{SDC_1}{SDC_1^{50\%}};\ a_1 + b_1 \leq z \leq a_2$$
$$\beta_2 = \frac{SDC_2 - SDC_1}{SDC_2^{50\%}};\ z \geq a_2 + b_2 \quad (13)$$

Finally, the damage severities are derived as:

$$\alpha_i = \frac{\beta_i}{1+\beta_i};\ i = 1,2 \quad (14)$$

In practice, the slope of deflection change at one location can be approximately calculated from the measured *DC* vector by:

$$SDC(z) = \frac{DC(z+\Delta z) - DC(z)}{\Delta z};\ z \geq a+b, \Delta z > 0 \quad (15)$$

Theoretically, *SDC(z)* is a constant function in the undamaged regions. However, under the presence of measurement noise, certain variations of the *SDC(z)* at different *z* locations is unavoidable. Therefore, in practice, the average $\overline{SDC_i}$ and $\overline{SDC_i}^{50\%}$ terms should be used in (13).

2.2 Obtaining Static Deflections

For damage detection purposes, structural deflections can be measured directly for the case the applied loads are known [5], or estimated indirectly from modal flexibility matrices constructed from vibration characteristics [17, 21]. To examine the performance of the proposed DI approach in CG dams, in this study, numerical investigations will be conducted on a FE model under two separated load cases: (i) operational loads including hydrostatic pressure and the dam self-weight, and (ii) virtual unit point load acting at the dam crest. Deflection under the first load case is extracted directly from the FE model and can represent the actual static deflection measurement. By contrast, as the unit point load acting at the dam crest is not a real load case, the corresponding deflection is obtained indirectly from the measured modal flexibility (MF) matrices. The process of obtaining the MF-based deflections is briefly described as follows. The flexibility matrix *F* can be well approximated from a few lower modes of vibration as follows [22]:

$$F = \sum_{i=1}^{m}\frac{1}{\omega_i^2}\phi_i\phi_i^T \quad (16)$$

where, ϕ_i and ω_i are the i^{th} mass-normalized mode shape and modal frequency, respectively; *m* is the number of the measured or interested modes, which is normally much lower than the degrees of freedoms (DOFs) of the system. After obtaining the MF matrix, the deflection of the structure under an arbitrary equivalent static point load **f** can be estimated by:

$$u = F\,\boldsymbol{f} \quad (17)$$

For a single unit point load acting at the dam crest, the deflection vector is generally the column of the MF matrix corresponding to the dam crest translational DOF.

3 NUMERICAL INVESTIGATIONS

In this section, the feasibility of the proposed approach will be examined through numerical study. However, due to page limit, only the capability of the approach in detecting and locating the damage is investigated using changes in the deflection change

DC parameter. Full investigations including the use of the *SDC* parameter in quantifying the located damage will be presented in future works of the authors.

3.1 Finite Element Model

The Koyna CG dam is one of a few popular concrete dams that experienced severe seismic cracking due to earthquakes. A comprehensive report on the damage patterns of the dam and the earthquake characteristics is presented in Chopra and Chakrabarti [23]. In the present study, the 103-meter high tallest non-overflow cross section of the dam is modelled using 2D plane stress elements in the ABAQUS finite element software (Figure 5-a). For simplicity, the dam is assumed to be fixed at its base and subjected to its self-weight and hydrostatic pressure when the earthquake occurred. The assumed elastic material properties E=31027 MPa, ν=0.2 and mass density = 2643 kg/m^3, and the first four natural periods of the model T_1 = 0.326 sec, T_2=0.124 sec, T_3=0.090 sec, and T_4=0.063 sec, are consistent with those reported in the literature [23, 24]. The tensile and compressive strength of the concrete are taken to be 2.9 MPa and 24.1 MPa, respectively.

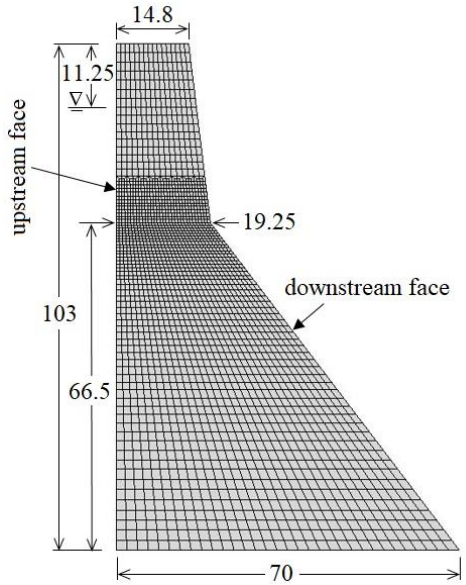

Figure 4. Finite element model of Koyna dam (after Bhattacharjee and Leger [24])

The Koyna earthquake accelerations (Figure 5-b) were assigned to the dam model at its base to simulate the actual seismic forces. Several damage scenarios were created by applying different scaling factors to the input earthquake accelerations resulting in different transverse peak ground acceleration (PGA) values (Table 1). The plastic-damage constitutive model for concrete subjected to cyclic loads developed by Lee and Fenves [25] was used to simulate crack initiation and propagation. Figure 6 illustrates the damaged regions, which are relevant to experimental and numerical studies in the literature (Figure 7), such as Mridha and Maity [26], Wang *et al*, [27]. In Figure 6, the damaged (cracked) regions are determined where the tensile damage variable (named by ABAQUS as DAMAGET [28]) is close to 1. The figure indicates that cracks initiated at the dam neck from the damage case D1, then at the dam base from the damage case D2, before they penetrated into the dam body in the subsequent damage scenarios. The modal frequencies of the first four modes in the undamaged and the four damaged states are summarized in Table 2.

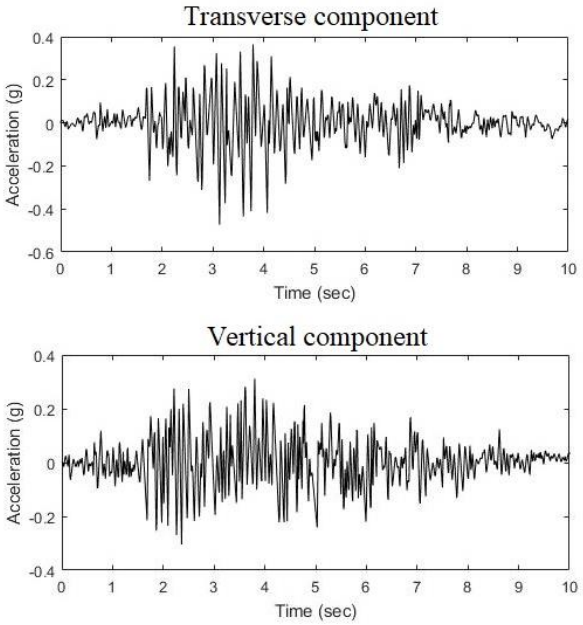

Figure 5. The Koyna earthquake accelerograms (after Bhattacharjee and Leger [24])

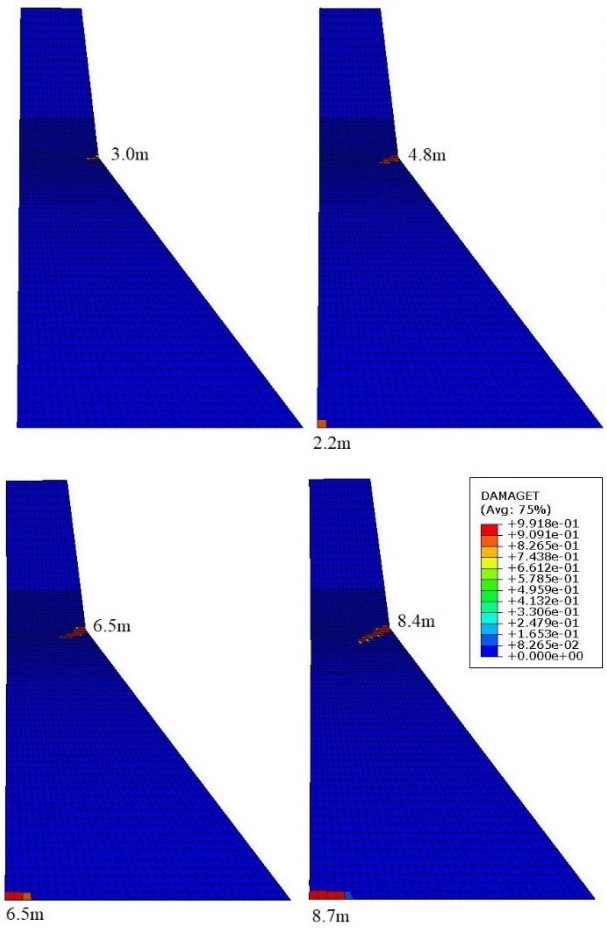

Figure 6. Damage scenarios with crack lengths (left to right, top to down: D1, D2, D3, D4)

Table 1. Damage scenarios

Damage case	D1	D2	D3	D4
PGA (g) of the transverse component	0.23	0.27	0.3	0.35
Crack length at dam neck (m)	3.0	4.8	6.5	8.4
Crack length at dam base (m)	-	2.2	6.5	8.7

The trend of reductions in the natural frequency throughout the damage scenarios clearly indicates the presence of cumulative damage. However, further investigations are needed to identify the damage.

Figure 7. Experimental simulation of cracks under on a Koyna dam model [26]

Table 2. Natural frequencies in different damaged states (units: Hz)

Mode No.	D0	D1	D2	D3	D4
1	3.066	3.062	3.055	3.044	3.035
2	8.097	8.082	8.056	8.004	7.964
3	11.073	11.068	11.057	11.033	11.000
4	15.906	15.901	15.884	15.818	15.713

Note: "D0" in Table 2 denotes the undamaged state.

3.2 Damage Identification from Deflection Change under Operational Loads

Figure 8 compares typical dam deformations under its self-weight and the hydrostatic loads before and after the occurrence of damage due to earthquake. It shows that for the lower portion below the dam neck, the cracks occurs at the dam base from the upstream surface caused additional deflection towards the downstream under high hydrostatic pressure. By contrast, for the upper portion of the dam, since the hydrostatic pressure is significantly smaller, the seismic cracks develop and open from the downstream at the dam neck level caused additional deflection towards the upstream under the dam self-weight.

The deflections of the dam are extracted for the upstream (US) and downstream (DS) faces in order to calculate the *DC* vectors, which are plotted in Figure 9 and Figure 10. For the damage case D1, from the dam base upwards, the *DC* plot encompasses a zero portion, before it linearly increases towards the US direction. According to the developed damage locating concept, the region between these two linear portions (around z = 66.5m) is correctly identified as damage. Similar damage patterns are found in the *DC* plots of the remaining damage cases, but with different inclination of the linear portions. For the crack at the dam base, though it initiated from D2, it might not be significant enough to be detected until becoming more severe in the damage cases D3 and D4. In these two last scenarios, the *DCs* in the lower part of the dam inclines towards the DS direction, indicating the presence of damage at the dam base.

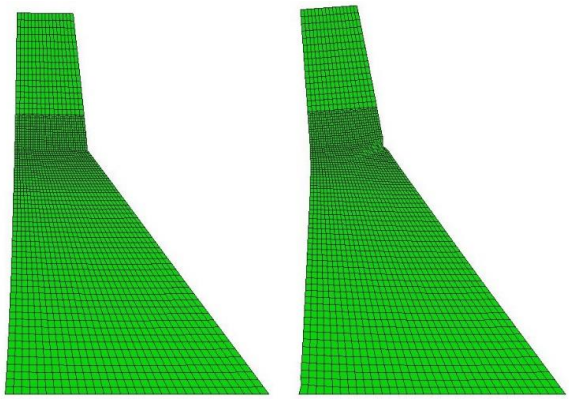

Figure 8. Deformation of the dam under operational loads (Undamaged left and D4 right; deformation scale factor: 1000)

It can also be observed from Figure 9 and Figure 10 that the slope of the *DC* plots in the linear portions gradually increases as the cracks propagated deeper into the dam body. Therefore, the proposed DI method can be used to monitor the development of the damage.

By observing the *DC* plot, the maximum magnitude of *DC* at the highest point of the dam ranges from 0.5mm to 4mm. This is within the measurable range of current deflection measurement techniques that can record the deflections to the unit of 0.1mm [29].

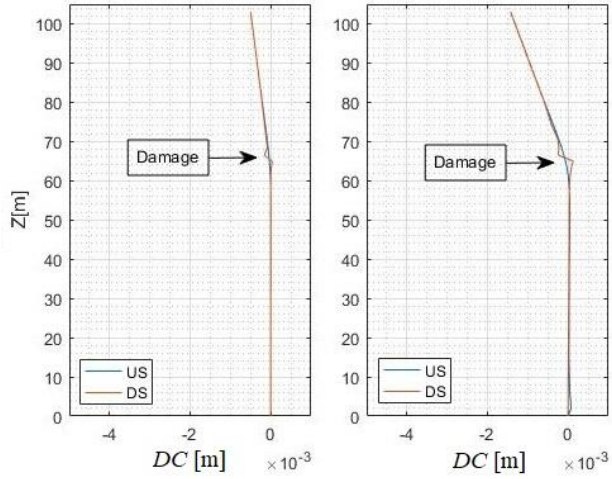

Figure 9. Deflection change plots under operational loads (left to right: D1, D2)

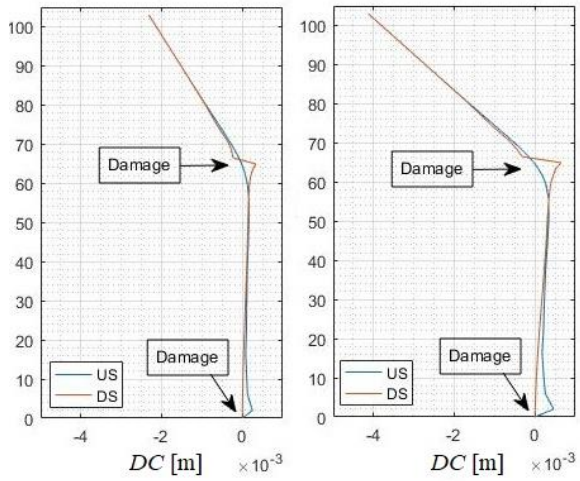

Figure 10. Deflection change plots under operational loads (left to right: D3, D4)

3.3 Damage Identification from Modal Flexibility-Based Deflection Change

In this section, the deflections under a virtual unit point load acting at the dam crest are estimated indirectly from the MF matrices, which are constructed from only the first mode of vibration. The resultant MF-based *DC* plots of the four damage scenarios are presented in Figure 11 and Figure 12. As expected, the MF-based *DC* plots follow the theoretical *DC* pattern, which clearly reveal the cracked regions at the dam neck and base. Similar to the DI results in the previous section, the method experiences difficulty in detecting early cracks at the dam base (D2). One distinctiveness compared to the *DC* plots under the operational loads is that the MF-based *DC* plots continuously increase towards the downstream direction in the upper part of the dam. This is because the MF-based *DC* indicates global cumulative increases in the flexibility of the dam above the damage locations.

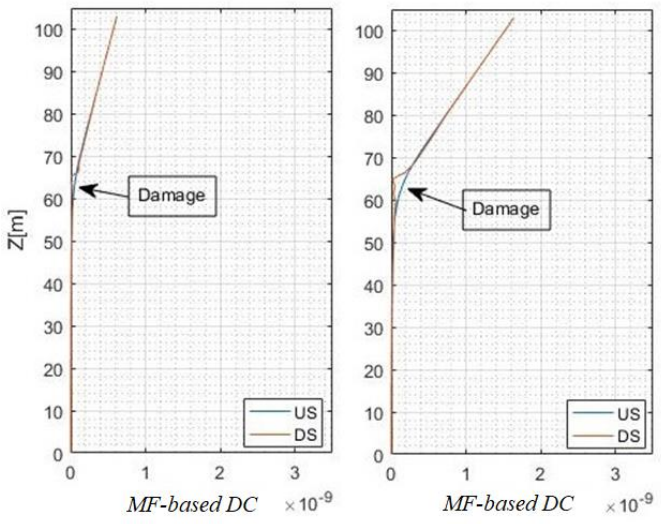

Figure 11. MF-based deflection change plots under virtual unit point load (left to right: D1, D2)

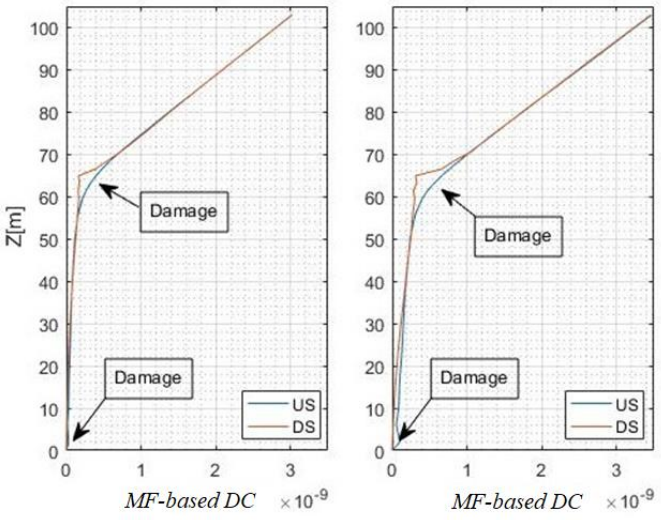

Figure 12. MF-based deflection change plots under virtual unit point load (left to right: D3, D4)

4 CONCLUSIONS

In this paper, an approach to locate and quantify damage in CG dams from changes in static deflection and modal parameters is presented. The development of the damage identification method is based on a theoretical static deflection change pattern developed for cantilever Timoshenko beams taken into account both flexural and shear effects. Numerical investigations indicate that the proposed method can accurately locate various seismic crack scenarios, which can be seen as a common damage type in CG dams.

The proposed approach can be applicable for the case where static deflections are measured directly under known static load such as hydrostatic pressure from the reservoir. Alternatively, it is demonstrated that the use of indirect MF-based deflections estimated from modal flexibility matrix would bring satisfactory damage detection results.

As the paper is mostly centered around the feasibility investigation of the method, further research is needed and may be reported in the future work of the authors.

REFERENCES

1. De Wrachien, D. and S. Mambretti, *Dam-break problems, solutions and case studies*. 2009: WIT press.
2. Chan, T. and D.P. Thambiratnam, *Structural health monitoring in Australia*. 2011, New York: Nova Science Publishers.
3. Sohn, H., C.R. Farrar, F.M. Hemez, D.D. Shunk, D.W. Stinemates, B.R. Nadler, and J.J. Czarnecki, *A review of structural health monitoring literature: 1996-2001*. 2004: Los Alamos National Laboratory Los Alamos, NM.
4. Karbhari, V.M. and F. Ansari, *Structural health monitoring of civil infrastructure systems*. 2009: Elsevier.
5. Le, N.T., D. Thambiratnam, A. Nguyen, and T.H. Chan, *A new method for locating and quantifying damage in beams from static deflection changes.* Engineering Structures, 2019. **180**: p. 779-792.
6. Doebling, S.W. and C.R. Farrar. *Computation of structural flexibility for bridge health monitoring using ambient modal data*. in *Proceedings of the 11th ASCE Engineering Mechanics Conference*. 1996. Ft. Lauderdale, FL, USA: Citeseer.
7. Ni, Y., H. Zhou, K. Chan, and J. Ko, *Modal Flexibility Analysis of Cable-Stayed Ting Kau Bridge for Damage Identification.* Computer-Aided Civil and Infrastructure Engineering, 2008. **23**(3): p. 223-236.
8. Jayasundara, N., D. Thambiratnam, T. Chan, and A. Nguyen, *Damage detection and quantification in deck type arch bridges*

using vibration based methods and artificial neural networks. Engineering Failure Analysis, 2020. **109**: p. 104265.
9. OBrien, E., C. Carey, and J. Keenahan, *Bridge damage detection using ambient traffic and moving force identification.* Structural Control and Health Monitoring, 2015. **22**(12): p. 1396-1407.
10. Koo, K., S.-H. Sung, and H.-J. Jung, *Damage quantification of shear buildings using deflections obtained by modal flexibility.* Smart Materials and Structures, 2011. **20**(4): p. 045010.
11. Bernagozzi, G., S. Mukhopadhyay, R. Betti, L. Landi, and P.P. Diotallevi, *Output-only damage detection in buildings using proportional modal flexibility-based deflections in unknown mass scenarios.* Engineering Structures, 2018. **167**: p. 549-566.
12. Wang, Y., D.P. Thambiratnam, T.H. Chan, and A. Nguyen, *Method development of damage detection in asymmetric buildings.* Journal of Sound and Vibration, 2018. **413**: p. 41-56.
13. Le, N.T., D.P. Thambiratnam, T.H.T. Chan, A. Nguyen, and B.K.T. Huynh. *Damage assessment of concrete gravity dams using vibration characteristics*. in *6th International Conference on Structural Engineering, Mechanics and Computation, SEMC*. 2016.
14. Cheng, L., J. Yang, D. Zheng, B. Li, and J. Ren, *The Health Monitoring Method of Concrete Dams Based on Ambient Vibration Testing and Kernel Principle Analysis.* Shock and Vibration, 2015. **2015**: p. 1-11.
15. Boumechra, N., *Damage detection in beam and truss structures by the inverse analysis of the static response due to moving loads.* Structural Control and Health Monitoring, 2017. **24**(10).
16. Le, N.T., D.P. Thambiratnam, T.H.T. Chan, and A. Nguyen. *Damage quantification in beam-like structures from modal flexibility change*. in *SHMII 2017 - 8th International Conference on Structural Health Monitoring of Intelligent Infrastructure, Proceedings*. 2017.
17. Le, N.T., A. Nguyen, D. Thambiratnam, T. Chan, and T. Khuc, *Locating and quantifying damage in beam-like structures using modal flexibility-based deflection changes.* International Journal of Structural Stability and Dynamics, 2020. **20**.
18. Wu, Z. and H. Su, *Dam health diagnosis and evaluation.* Smart Materials and Structures, 2005. **14**(3): p. S130-S136.
19. Loh, C.-H. and T.-S. Wu, *Identification of Fei-Tsui arch dam from both ambient and seismic response data*. Soil Dynamics and Earthquake Engineering, 1996. **15**(7): p. 465-483.
20. Bukenya, P., P. Moyo, H. Beushausen, and C. Oosthuizen, *Health monitoring of concrete dams: A literature review.* Journal of Civil Structural Health Monitoring, 2014. **4**(4): p. 235-244.
21. Sung, S., K. Koo, and H. Jung, *Modal flexibility-based damage detection of cantilever beam-type structures using baseline modification.* Journal of Sound and Vibration, 2014. **333**(18): p. 4123-4138.
22. Pandey, A.K. and M. Biswas, *Damage detection in structures using changes in flexibility.* Journal of Sound and Vibration, 1994. **169**(1): p. 3-17.
23. Chopra, A.K. and P. Chakrabarti, *The earthquake experience at Koyna dam and stresses in concrete gravity dams.* Earthquake Engineering & Structural Dynamics, 1972. **1**(2): p. 151-164.
24. Bhattacharjee, S. and P. Leger, *Seismic cracking and energy dissipation in concrete gravity dams.* Earthquake engineering & structural dynamics, 1993. **22**(11): p. 991-1007.
25. Lee, J. and G.L. Fenves, *A plastic-damage concrete model for earthquake analysis of dams.* Earthquake engineering & structural dynamics, 1998. **27**(9): p. 937-956.
26. Mridha, S. and D. Maity, *Experimental investigation on nonlinear dynamic response of concrete gravity dam-reservoir system.* Engineering Structures, 2014. **80**: p. 289-297.
27. Wang, G., Y. Wang, W. Lu, C. Zhou, M. Chen, and P. Yan, *XFEM based seismic potential failure mode analysis of concrete gravity dam–water–foundation systems through incremental dynamic analysis.* Engineering Structures, 2015. **98**: p. 81-94.
28. Simulia. *Abaqus 6.14 Documentation*. 2014; Available from: http://130.149.89.49:2080/v6.14/.
29. Lew, J.-S. and C.-H. Loh, *Structural health monitoring of an arch dam from static deformation*. Journal of Civil Structural Health Monitoring, 2014. **4**(4): p. 245-253.